ChemPubSoc Europe

DOI: 10.1002/slct.201700793

Chemistry SELECT Full Papers

Analytical Chemistry

In–Vitro Development and Characterisation of a Superoxide Dismutase-Based Biosensor.

Michelle M. Doran,* Niall J. Finnerty, and John P. Lowry*[a]

A first generation amperometric biosensor for the detection of superoxide (O_2^-) was constructed utilising a dip-coating approach for immobilising the enzyme superoxide dismutase (SOD, 200 U/mL) onto a Pt electrode. Several dip-coating procedures were investigated, incorporating styrene, glutaraldehyde, bovine serum albumin and polyethylenimine at various concentrations, in order to develop a simple and reproducible coating method to maximise the sensitivity of the sensor to O_2^-. The optimised design was produced using 5 dip-coatings and a composite containing 200 U/mL SOD, 0.5% glutaraldehyde and 2% polyethylenimine (Sty-(SOD-0.5%GA-2%PEI)$_5$). This sensor displayed excellent permselective characteristics with negligible signals produced by 12 of the most common electroactive species present in brain extracellular fluid, including uric acid (UA) which is produced as a by-product of the O_2^- generating xanthine-xanthine oxidase calibration method. In addition, it had a response time of *ca.* 1 s, high sensitivity to O_2^- (0.91 ± 0.02 nA/μM), and an *in-vitro* limit of detection of *ca.* 0.063 μM, thus suggesting potential use for neurochemical monitoring of O_2^- *in-vivo*.

Introduction

The biological reactive oxygen species (ROS) superoxide (O_2^-) is generated as a reduced intermediate of molecular oxygen (O_2).[1,2] Its major source in cells is electron 'leakage' from electron transport chains in the mitochondria and in the endoplasmic reticulum.[3] Under normal metabolic conditions ROS are produced at a rate which is matched by the capacity of tissues to catabolise them.[4,5] However, when their production exceeds the body's natural ability to deal with this potentially cytotoxic process, a variety of pathological conditions may occur, including stroke, cancer and neurodegeneration.[6,7] This is true for O_2^- which under normal physiological conditions has a very low nanomolar concentration (10–100 nM)[8] due to the natural ability of superoxide dismutase (SOD) to catalyse its dismutation and its high reactivity with other small molecules.[9,10]

Several techniques for measuring the concentration of O_2^- indirectly are currently available including electron spin resonance (ESR),[11–13] chemiluminescence[14–17] or certain semiquantitative colorimetric tests. However, none of these are suitable for direct monitoring in biological tissues and recently electrochemical techniques have become popular in order for direct real-time monitoring of O_2^-. Several first,[18,19] second[20,21] and third generation[22–26] O_2^- biosensors have been developed for O_2^- monitoring. These sensors have utilised various transducers including Pt, Au and carbon fibre and various immobilisation techniques. The most common methods of immobilisation include entrapment within a membrane, cross-linking, covalent bonding and physical adsorption.[27–29] Few reports exist for measuring O_2^- levels *in-vivo* in freely-moving animals because of its low concentration, fleeting existence and high reactivity in the *in-vivo* environment. For a number of years, *in-vivo* electrochemistry has been used for the detection of substances in the living brain.[30,31] Our goal here is to utilise previous experience to develop a SOD-based biosensor for real-time neurochemical monitoring of O_2^- *in-vivo*.

In this paper, we report the development of a first generation biosensor immobilising the enzyme SOD on a Pt electrode. In order to generate O_2^- in the electrochemical cell this biosensor utilises the classical xanthine-xanthine oxidase (XOD) reaction.[32] XOD catalyses the univalent and divalent reduction of molecular O_2 generating O_2^- and hydrogen peroxide (H_2O_2)[33] resulting in the oxidation of xanthine to uric acid (UA) as shown below;

$$\text{Xanthine} + H_2O + O_2 \xrightarrow{XOD} UA + O_2^- + 2H^+$$

The SOD immobilised on the electrode surface then catalyses the dismutation reaction of the O_2^- radical with the production of O_2 and H_2O_2;

$$2H^+ + 2O_2^- \xrightarrow{SOD} H_2O_2 + O_2$$

The H_2O_2 generated from this enzymatic process is oxidised at the electrode surface producing the signal generating current;

$$H_2O_2 \rightarrow 2H^+ + O_2 + 2e^-$$

We initially utilised a dip-coating approach to create a composite layer of enzyme and stabilising agents in order to

[a] *Dr. M. M. Doran, Dr. N. J. Finnerty, Prof. J. P. Lowry*
Neurochemistry Laboratory, Maynooth University Department of Chemistry, Maynooth University, Maynooth, Co. Kildare, Ireland
,
E-mail: Michelle.Doran@nuim.ie
John.Lowry@nuim.ie

Supporting information for this article is available on the WWW under https://doi.org/10.1002/slct.201700793

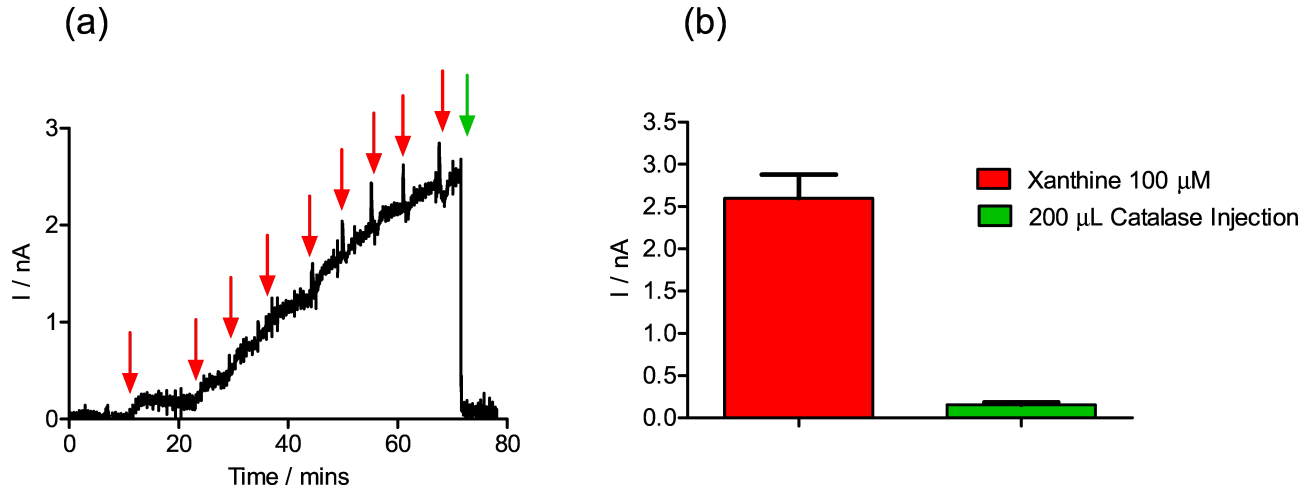

Figure 1. (a) Typical raw data trace for a xanthine-XOD calibration on a Pt-PPD sensor. The red arrows indicate sequential 1, 3, 6, 10, 20, 40, 60, 80 and 100 µM xanthine injections. The green arrow indicates a 200 µL injection of catalase. Calibration performed using CPA at +700 mV *vs.* SCE. **(b)** Bar chart showing the current comparison between $I_{100\ \mu M}$ xanthine (2.597 ± 0.28 nA, n = 6) prior to a 200 µL injection of catalase on Pt-PPD sensors. The introduction of catalase resulted in an instantaneous decrease in current to baseline (0.154 ± 0.028 nA, n = 6).

maximise sensitivity. This is critical in order to enable physiological monitoring of O_2^- due to its nanomolar concentrations. In addition, we incorporated a permselective layer of poly-*o*-phenylenediamine (PPD) which facilitated high permeability to the enzyme generated H_2O_2[34,35] and effective rejection of the UA produced by the oxidation of xanthine in the *in-vitro* calibration process. This layer also eliminated signals from several endogenous interferent species including ascorbic acid (AA).[36,37] The resultant fast responding, highly selective and sensitive biosensor has the potential for use in neurochemical monitoring of O_2^- *in-vivo*.

Results and Discussion

Interferents in Superoxide Calibration

The O_2^- radical is generated by the oxidation of xanthine to UA in the presence of XOD. However, UA is electroactive at the applied potential of +700 mV and therefore, its contribution to the biosensor's signal must be minimised. The inclusion of the permselective PPD layer prior to modification with the immobilising/stabilising components resulted in a significant decrease ($P < 0.0001$) in the current recorded on addition of 100 µM xanthine: 41.13 ± 3.22 nA (Bare Pt, n = 30) to 2.02 ± 0.17 nA (Pt-PPD, n = 16). This result confirms that the UA current was effectively eliminated by incorporation of the PPD layer.

Additionally, the spontaneous dismutation of O_2^- to H_2O_2 in the presence of excess H^+ ions is another potential source of interference which was verified by injecting a single 200 µL aliquot of catalase into the electrochemical cell after the addition of 100 µM xanthine. This produced an instantaneous decrease in current to baseline levels (see Figure 1(a) and (b)) suggesting that the spontaneous dismutation of O_2^- is taking place in the electrochemical cell.

O_2^- dismutation by SOD is first order with respect to O_2^- concentration whereas the spontaneous dismutation is second order, with a pH dependent second order rate of ~ 10^5 $M^{-1}s^{-1}$ at pH 7.0.[38] The enzyme used in the development of this biosensor Cu,Zn SOD accelerates the destruction of O_2^- increasing the rate constant of the dismutation reaction to 2 x 10^9 $M^{-1}s^{-1}$.[39] This suggests that SOD is more efficient at accelerating the decomposition of O_2^- compared with the spontaneous dismutation, at low concentrations, therefore suggesting that the enzymatic dismutation of O_2^- is more favourable than the spontaneous dismutation of O_2^- in the electrolyte.

However, despite the need to eliminate the spontaneous dismutation few reports exist which distinguish this H_2O_2 from that generated by the enzymatic SOD reaction. Few research groups have manufactured first generation biosensors for the detection of SOD generated H_2O_2 which employ specific techniques to differentiate this H_2O_2 from the H_2O_2 produced by spontaneous dismutation. McNeil and co-workers developed a O_2^- biosensor based on SOD-coated platinised carbon electrodes (PACE). The SOD-coated biosensor was polarised at +320 mV *vs.* Ag/AgCl to estimate the H_2O_2 produced by the enzyme disproportionation of O_2^- through its oxidation current. Similarly, this biosensor uses a subtraction method to eliminate the current generated due to the natural disproportionation of O_2^- measured using a second electrode which consisted of bovine serum albumin (BSA) coated PACE.[40]

Effect of Enzyme Concentration

Synthetic polymers such as styrene and methyl methacrylate have been successfully used as enzyme immobilisers in the manufacture of biosensors for neurochemical monitoring. Both are liquids at room temperature and thus provide a convenient method for the entrapment of SOD using the dip-coating

Table 1. A comparison of V_{max}, K_m and LRS for designs 1–16 using varying concentrations of SOD and biosensor components GA, BSA and PEI. The subscript represents the number of 1 second dips into the SOD solution and various biosensor constituents.

Design	Composition	n	V_{max} nA	K_m μM	LRS nA/μM
1	*Sty-(SOD(200U))$_1$*	4	2.43 ± 0.13	7.57 ± 1.51	0.13 ± 0.004
2	*Sty-(SOD(200U))$_2$*	4	8.56 ± 0.12	9.08 ± 0.42	0.41 ± 0.02
3	*Sty-(SOD(200U))$_5$*	8	5.65 ± 0.24	15.47 ± 0.54	0.52 ± 0.02
4	*Sty-(SOD(200U))$_{10}$*	4	4.77 ± 0.07	5.08 ± 0.30	0.30 ± 0.03
5	*Sty-(SOD(100U)$_5$*	12	7.40 ± 0.10	6.86 ± 0.31	0.41 ± 0.03
6	*Sty-(SOD(400U)$_5$*	12	7.53 ± 0.13	8.28 ± 0.46	0.35 ± 0.03
7	*Sty-(SOD-0.5 %GA)$_5$*	8	5.42 ± 0.06	6.87 ± 0.25	0.42 ± 0.01
8	*Sty-(SOD-1 %BSA-0.5 %GA)$_5$*	6	10.33 ± 0.5	15.02 ± 1.46	0.34 ± 0.02
9	*Sty-(SOD-0.5 %GA-2 %PEI)$_5$*	17	15.98 ± 0.15	10.33 ± 0.27	0.91 ± 0.02
10	*Sty-(SOD-0.5 %GA-1 %PEI)$_5$*	12	10.05 ± 0.10	6.09 ± 0.22	0.85 ± 0.04
11	*Sty-(SOD-0.5 %GA-3 %PEI)$_5$*	11	72.76 ± 6.25	100.30 ± 15.26	0.63 ± 0.03
12	*Sty-(SOD-0.05 %GA-2 %PEI)$_5$*	8	60.08 ± 5.56	104.70 ± 20.34	0.63. ± 0.01
13	*Sty-(SOD-1 %GA-2 %PEI)$_5$*	7	40.38 ± 1.90	45.90 ± 4.50	0.51 ± 0.01
14	*Sty-(SOD-1 %BSA-0.5 %GA-2 %PEI)$_5$*	12	12.82 ± 0.14	21.82 ± 0.53	0.28 ± 0.01
15	*Sty-(SOD-0.1 %BSA-0.5 %GA-2 %PEI)$_5$*	12	5.53 ± 0.06	4.71 ± 0.21	0.70 ± 0.04
16	*Sty-(SOD-0.01 %BSA-0.5 %GA-2 %PEI)$_5$*	9	19.53 ± 0.49	21.17 ± 1.30	0.61 ± 0.04

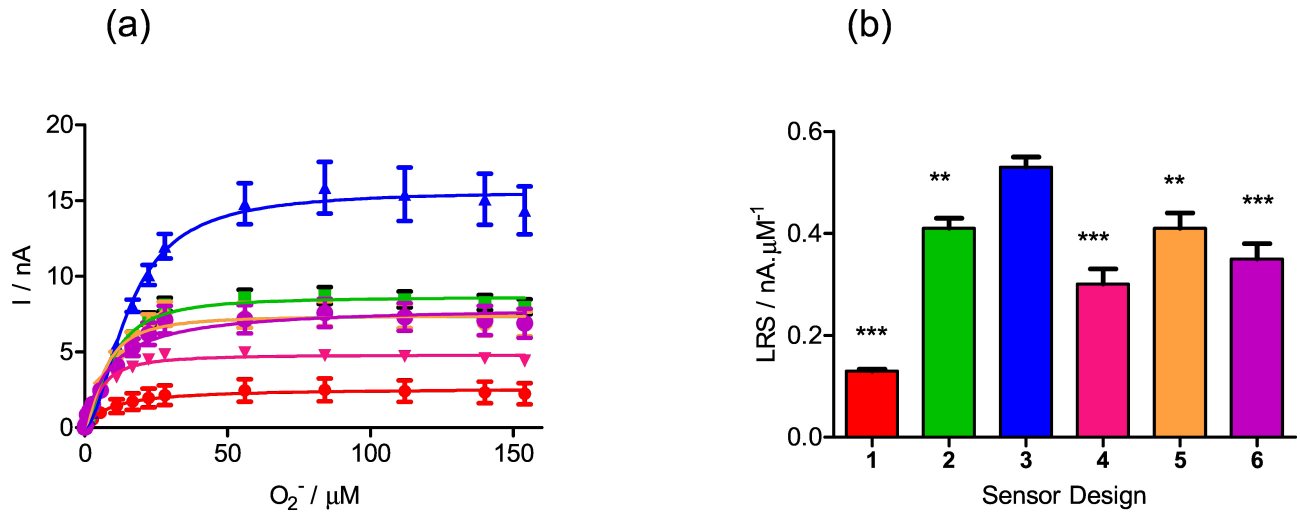

Figure 2. (a) The current-concentration profiles for O_2^- calibrations (0-154 μM) for biosensor designs 1 (red), 2 (green), 3 (blue), 4 (pink), 5 (orange) and 6 (purple) calibrated in PBS (pH 7.4) buffer solution containing 0.002 U XOD at 21 °C. Calibrations performed using CPA at +700 mV *vs.* SCE. **(b)** Bar chart comparing sensitivities (Linear Region Slope, nA/μM) for biosensor designs 1–6. *p < 0.05; **p < 0.01; ***p < 0.001 *vs.* Design 3, unpaired Students t-test.

approach to enzyme loading[41] on the Pt surface. Also, it has recently been reported that styrene and methyl methacrylate facilitate increased active enzyme loading in biosensors designed for neurochemical monitoring.[42]

Designs 1–4 demonstrate the successful immobilisation of SOD (200 U/mL) by entrapment within a styrene layer on a Pt 1 mm cylinder surface. Table 1 highlights the differences in the kinetic parameters for each of the four designs tested with Figure 2(a) showing the Michaelis-Menten plots generated on addition of xanthine (0–550 μM) for each of the designs. Design 3 (see Figure 2(b)) displayed a significant improvement in sensitivity (0.53 ± 0.02 nA/μM, n = 8) when compared to design 1 (0.13 ± 0.004 nA/μM (n = 4), P < 0.0001), design 2 (0.41 ± 0.02 nA/μM (n = 4), P = 0.0037) and design 4 (0.30 ± 0.03 nA/μM (n = 4), P < 0.0001).

In designs 5 and 6 we investigated the effect of changing the concentration of the enzyme solution. The unit of activity was decreased to 100 U/mL (design 5) and increased to 400 U/mL (design 6). The ideal enzyme unit of activity was determined to be 200 U/mL (design 3, see Figure 2(b)) as it produced a high V_{max} current of 15.65 ± 0.24 nA, a K_m concentration of 15.47 ± 0.54 μM and a significant increase in sensitivity when compared to design 5 (0.41 ± 0.03 nA/μM (n = 12), P = 0.0082) and design 6 (0.35 ± 0.03 nA/μM (n = 12), P = 0.0003). All further design modifications thus utilised 5 layers of 200 U SOD.

Optimisation of Biosensor Design

The addition of a cross-linking agent such as glutaraldehyde has been utilised regularly in the construction of biosensors to improve enzyme stability.[43,44] Glutaraldehyde usually cross-links with the lysine residues on the enzyme which are typically located on the protein surface rather than the catalytic site,

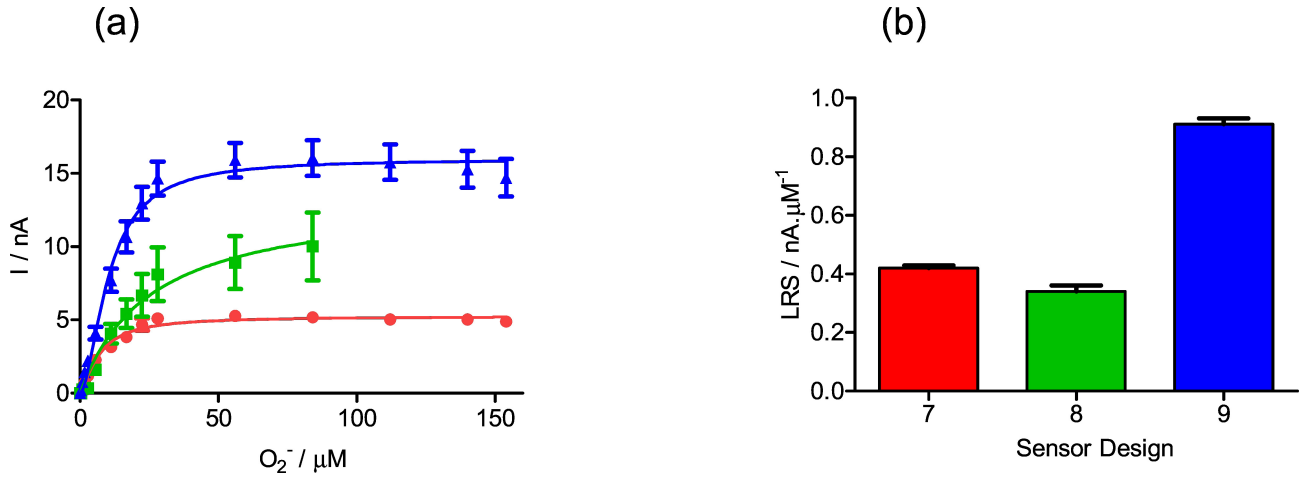

Figure 3. (a) The current-concentration profiles for O_2^- calibrations (0-154 μM) for biosensor designs 7 (red), 8 (green) and 9 (blue) calibrated in PBS (pH 7.4) buffer solution containing 0.002 U XOD at 21 °C. Calibrations performed using CPA at +700 mV *vs.* SCE. **(b)** Bar chart displaying a comparison of the sensitivities for biosensor designs 7–9.

therefore preserving the protein conformation. Design 7 incorporates glutaraldehyde (0.5%) and resulted in a decrease in the K_m concentration, V_{max} and sensitivity when compared to design 3 (see Table 1). The addition of BSA into a biosensor for L-Glutamic acid has previously been reported to protect the enzyme from inactivation during the polymerisation of the enzyme within a PPD film.[45] The inclusion of lysine rich BSA, 1% into design 8 (see Figure 3(a)) increased the K_m concentration to 15.02 ± 1.46 μM, (n = 6) and the V_{max} current to 10.33 ± 0.50 nA, (n = 6), however a significant decrease (P = 0.001) in sensitivity was observed (0.34 ± 0.02 nA/μM, n = 6) when compared to design 7. In this instance, the glutaraldehyde crosslinks the BSA in addition to the enzyme thus limiting the direct enzyme cross-linking, resulting in higher enzyme activity and stability.

The polybasic positively charged aliphatic amine polyethylenimine (PEI) has also been incorporated into biosensor designs for both immobilisation[46,47] and stabilisation.[48,49] The introduction of PEI has proven beneficial in the development of biosensors for its ability to increase the sensitivity[46] and reduce the Michaelis constant K_m.[50] These beneficial traits are attributed to the formation of polyanionic/polycationic complexes between the polycation PEI and the polyanionic enzyme which reduces the enzyme deactivation.[51] This can also decrease the electrostatic repulsion between the enzyme substrate and biosensor components,[46] thus leading to the formation of a stable configuration resulting in improved long-term stability of the biosensor. The inclusion of PEI (2%) in design 9 resulted in a significant increase ($P < 0.0001$) in sensitivity to 0.91 ± 0.02 nA/μM (n = 17) when compared to design 3 (0.52 ± 0.02 nA/μM, n = 8). This design also yielded a high V_{max} current of 15.98 ± 0.15 nA and a low K_m concentration of 10.33 ± 0.27 μM. Thus, all modified electrodes presented hereafter incorporate PEI into the design as its inclusion has resulted in a substantial increase in sensitivity when compared to designs 1–8.

Concentration Studies

The previous results observed for designs 1–9 demonstrate that SOD can be successfully immobilised on a Pt surface using the dip adsorption method. However, O_2^- has a low concentration *in-vivo* and consequently it was essential to investigate the concentration of the crosslinker and stablisiers in an attempt to improve the kinetic parameters and sensitivity further. The introduction of PEI resulted in a marked enhancement in the kinetic parameters and sensitivity, thus in designs 10 and 11 we investigated the impact of changing the PEI concentration to 1% and 3% respectively. Design 10 resulted in a decrease (P = 0.1554) in sensitivity to 0.85 ± 0.04 nA/μM, a significant decrease ($P < 0.0001$) in V_{max} to 10.05 ± 0.10 nA, and a significant ($P < 0.0001$) decrease in the K_m concentration to 6.09 ± 0.22 μM, when compared to design 9 incorporating the 2% concentration of PEI. Design 11 (3% PEI) produced poor enzyme kinetics and a high K_m concentration suggesting restricted access of the substrate to the active sites of the enzyme due to higher diffusional constraints.

Literature reports suggest that the amount of cross-linking agent used affects the degree or extent of cross-linking, with low concentrations of glutaraldehyde unable to form sufficient cross-linkages to effect precipitation of the enzyme.[52] Therefore, maintaining the PEI concentration at 2%, the glutaraldehyde concentration was changed to 0.05% (design 12) and 1% (design 13) in an attempt to improve the kinetic parameters. Both designs showed poor enzyme kinetics with high K_m concentrations of 104.70 ± 20.34 μM and 45.90 ± 4.50 μM respectively. A significant decrease ($P < 0.0001$ for both designs) in sensitivity was recorded when compared to design 9. Finally, the addition of BSA into sensor designs incorporating both GA and PEI was investigated. Three concentrations were utilised 1% (design 14), 0.1% (design 15) and 0.01% (design 16). The introduction of BSA resulted in a significant decrease in the sensitivity to 0.28 ± 0.008 nA/μM, (n = 12, $P < 0.0001$) for

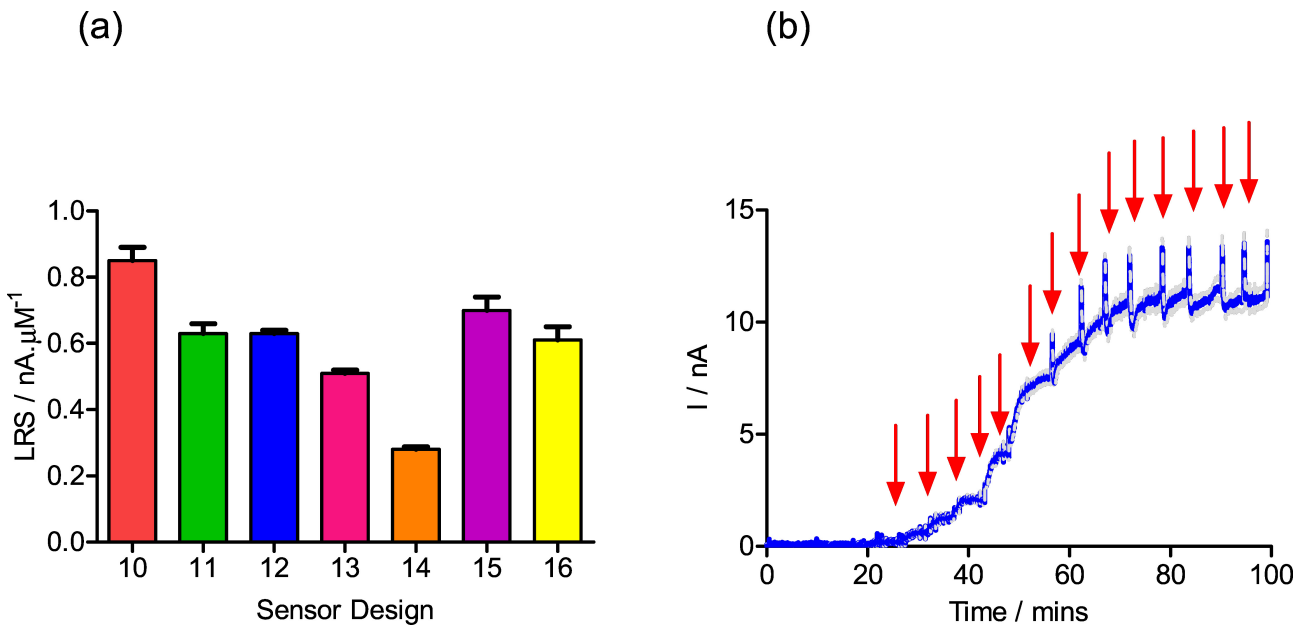

Figure 4. (a) Comparison of the average linear region slope for O_2^- biosensor designs 10–16. Linear region slope values were obtained from the Michaelis-Menten kinetic curve of the O_2^- calibrations (0 – 154 µM) performed using CPA at +700 mV *vs.* SCE in PBS (pH 7.4) buffer solution containing 0.002 U XOD. **(b)** Mean raw data trace for O_2^- calibration using design 10 (n = 4). Arrows indicate injections yielding concentrations of 0.28, 0.84, 1.68, 2.8, 5.6, 11.2, 16.8, 22.4, 28, 56, 84, 112, 140 and 154 µM O_2^-.

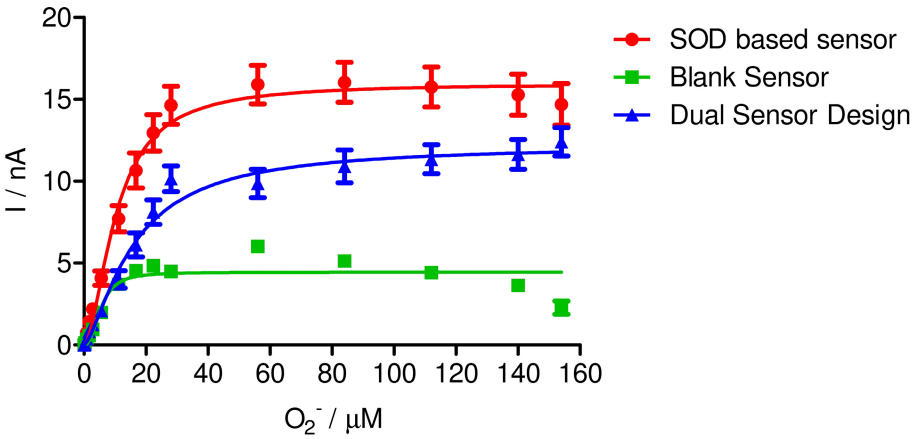

Figure 5. The current-concentration profiles for O_2^- calibrations performed in PBS (pH 7.4) buffer solution containing 0.002 U XOD at 21 °C for the SOD-based electrode (red), blank electrode (green) and dual sensor design (blue). CPA carried out at +700 mV *vs.* SCE.

design 14, 0.70 ± 0.04 nA/µM (n = 12, $P < 0.0001$) for design 15, and 0.61 ± 0.04 nA/µM (n = 9, $P < 0.0001$) for design 16.

Dual Sensor Configuration

As mentioned previously, O_2^- undergoes spontaneous dismutation in the electrolyte generating H_2O_2. However, this contribution can be eliminated using a dual sensor system. Design 9 demonstrated optimum kinetic parameters and recorded the highest sensitivity compared to other designs. It was therefore utilised in the dual sensor design to detect the spontaneously produced H_2O_2 and O_2^-. The second sensor (blank) incorporates no SOD but was modified with the relevant concentrations and layers of the other components, i.e. styrene, PEI and glutaraldehyde. A subtraction method was utilised in order to find a true representation of the concentration of O_2^- detected at the Pt surface and Figure 5 illustrates the dual sensor design in operation. A significant decrease ($P < 0.0001$) in current from 15.98 ± 0.15 nA (SOD-based electrode) to 2.29 ± 0.40 nA (blank electrode) was observed at 154 µM O_2^- (Figure 5).This indicates that the spontaneous dismutation of O_2^- accounts for ~ 2.30 nA of current generated at the O_2^- biosensor at 154 µM O_2^-. Similarly, a significant decrease ($P < 0.0001$) in sensitivity was observed from 0.91 ± 0.06 nA/µM (SOD-based electrode) to 0.33 ± 0.005 nA/µM (blank sensor). These results show that the production of H_2O_2 from the spontaneous dismutation accounts for only a small proportion of the signal when compared to the signal from the enzymatic dismutation. For future use *in-vivo*, the two electrodes will be implanted in close proximity to each other and the current from each will be

recorded simultaneously thus facilitating differential discrimination between the H_2O_2 signal due to the spontaneous dismutation of O_2^- and endogenously produced levels.

Limit of Detection and Time

The limit of detection (LOD) is an important parameter to consider when designing biosensors to monitor fast transients in brain analytes whose extracellular fluid (ECF) levels are invariably low. We calculated the LOD using three times the error on the lowest calibration concentration (0.28 μM) divided by the calibration slope (0.91 ± 0.07 nA/μM, Design 9). This gives a value of 0.063 ± 0.004 μM. In reality one can only use *in-vitro* calibration curves to guesstimate concentration changes *in vivo* due to differences in background currents and modifications to the electrode surface resulting from implantation.[53] Variations in signal *in-vivo* are usually represented as relative changes from background. As such, the LOD for *in-vivo* sensors is usually determined using the widely applied criterion of three times the standard deviation of the baseline signal[37,54,55] (0.026 ± 0.002 μM for Design 9). This range would suggest that it may be possible to monitor physiological changes associated with behavioural and/or pharmacological manipulations *in-vivo*. We also quantified the concentration determination error using the mean LRS to determine the calculated concentration for two standard additions (low and high, within the linear region) of 0.28 and 11.20 μM O_2^-. The values of 0.26 and 10.19 μM respectively are very similar to the standard values and represent a discrepancy of < 10%.

Response time, which is defined as the time taken for the response to rise from 10% to 90% of the maximum amplitude for a fixed concentration step (i.e. $t_{10\text{-}90\%}$), is difficult to separate from the mixing time in *in vitro* studies. Typical data for the O_2^- biosensor is shown in Figure 6 and it is clear that the response time is less than the mixing time and of the order of 1–2 seconds. This is similar to the response times reported for other Pt-based biosensors,[56,57] and is *ca.* 5 times faster than values reported for carbon-based biosensors.[55] Generally, in cases where the $t_{10\text{-}90\%}$ values are less than the mixing time *in-vitro*, we have found response times *in-vivo* in the millisecond range.[58–60]

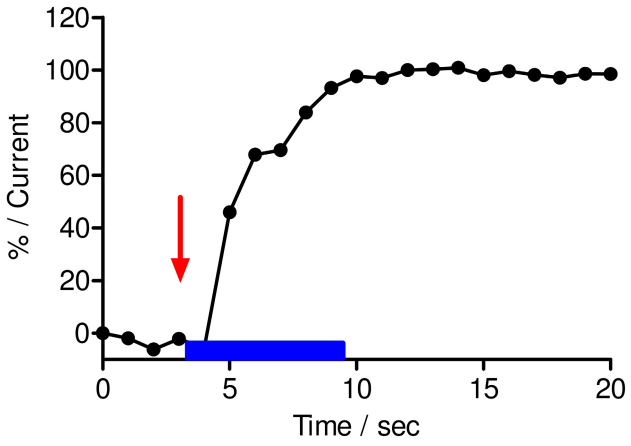

Figure 6. A typical example of a response time for a xanthine injection of 40 μM in PBS (pH 7.4) buffer solution at room temperature for the O_2^- biosensor. CPA carried out at +700 mV *vs.* SCE. Arrow indicates the point of injection and the blue rectangle symbolises the stirring time.

Interference Studies

The brain is anatomically complicated and contains a wide range of electroactive surfactants, electrode poisons, electrocatalysts and a tissue matrix that restricts mass transport to the electrode[31] as well as a large number of possible interfering species present at relatively high concentrations including AA, UA, and the catecholamines. The O_2^- radical has a very low endogenous concentration and therefore it is critical for the biosensor design to eliminate interferent signals while maintaining sufficient sensitivity for the target analyte. The optimised O_2^- biosensor (design 9) includes the polymer PPD in its construction for interference rejection. This polymer has previously been utilised in the development of biosensors for the detection of glucose,[59] H_2O_2[43] and D-serine,[61] and demonstrates beneficial traits such as being highly permeable to the enzyme generated H_2O_2[34] while effectively rejecting interferent species.[36] The selectivity of design 9 to a range of potential electroactive interferents present in the brain ECF was examined.

AA is considered the main electroactive interferent molecule present in the brain[62] and with an estimated basal concentration of 400 μM[63] could readily mask the signal from the nanomolar levels of O_2^-. Figure 7 shows the AA sensitivity recorded at the O_2^- biosensor as a function of varying AA concentration, and the mean current-concentration profile for

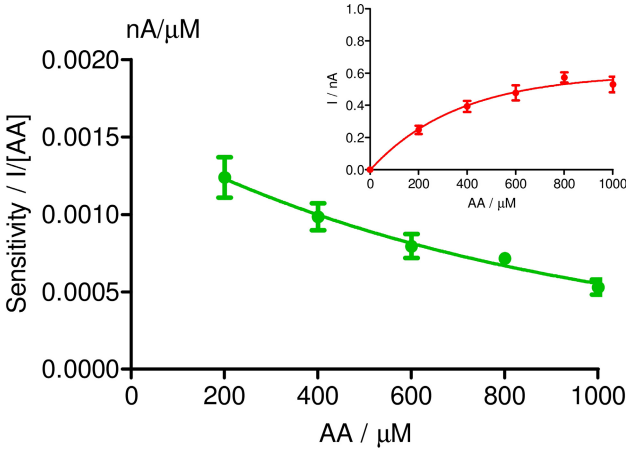

Figure 7. The sensitivity for the O_2^- biosensor as a function of AA concentration showing significant interference rejection and saturation characteristics at physiological levels. **Inset:** The mean current-concentration for AA calibrations (0-1000 μM) performed in N_2 saturated PBS (pH 7.4) at +700 mV (*vs.* SCE) and 21 °C using the O_2^- biosensor.

AA calibrations which shows saturation of the PPD layer resulting in a self-blocking phenomenon which has previously been reported.[36,35]

Other potential interferents tested (Table 2) included the monoamine neurotransmitters dopamine and 5-hydroxytryptomaine (5-HT), their metabolites 3,4-dihydroxyphenylacetic acid (DOPAC), homovanillic acid (HV) and 5-hydroxyindoleacetic acid (5-HIAA), dehydroascorbic acid (DHAA), the amino acids L-tyrosine, L–cysteine, L-tryptophan, the purine metabolite UA and the anti-oxidant glutathione.

Table 2. Results table for an interferent calibration showing the current response on addition of physiological levels of 11 interferent molecules.

Interferent	n	Concentration, μM	Current Response, nA	Signal as % of current at 0.84 μM O_2^-
L–Cysteine	3	50	0.089 ± 0.056	11.4%
L-Tyrosine	3	100	-0.050 ± 0.002	0%
UA	3	50	-0.074 ± 0.008	0%
Glutathione	3	50	-0.040 ± 0.004	0%
DHAA	3	100	-0.006 ± 0.001	0%
5-HIAA	3	50	-0.046 ± 0.016	0%
L-Tryptophan	3	100	-0.008 ± 0.005	0%
HVA	3	10	-0.012 ± 0.001	0%
Dopamine	3	0.05	-0.010 ± 0.000	0%
5-HT	3	0.01	0.003 ± 0.005	0.38%
DOPAC	3	20	0.002 ± 0.002	0.26%

Small negative currents (attributable to baseline drift) were obtained for most species suggesting no oxidation of the specific interferent. The administration of L-cysteine, 5-HT and DOPAC resulted in small negligible oxidation currents. Also, such signals would be further reduced through co-implantation with the blank sensor and differential signal analysis.

Conclusion

The detailed *in-vitro* development of a sensitive O_2^- biosensor is presented. The use of styrene as the immobilisation matrix facilitated the entrapment of SOD using the dip-coating approach to enzyme loading. The inclusion of the cross-linker glutaraldehyde and the stabiliser polyethylenimine produced a biosensor with excellent sensitivity to O_2^- and optimum kinetic parameters.

The electroactive interferents UA and the H_2O_2, produced from the spontaneous dismutation of O_2^-, contribute to the electrochemical signal unless eliminated successfully. The electropolymerisation of *o*-PD onto the Pt surface provided a successful method to negate the UA contribution without impacting negatively on the O_2^- sensitivity. A dual sensor design involving the SOD-based electrode (Sty-(SOD-GA-PEI)$_5$) and a blank sensor (Sty-(GA-PEI)$_5$) was employed to deal with the spontaneous dismutation interference. We also demonstrated the successful rejection of a range of other key endogenous interferent species such as AA, dopamine and metabolites. The resultant fast responding, highly selective and sensitive biosensor has the potential for use in neurochemical monitoring of O_2^- *in-vivo*.

Supporting Information Summary

The experimental section (materials and methods, working electrode preparation, instrumentation and data analysis, and sensor calibration) can be found in the Supporting Information.

Acknowledgements

We gratefully acknowledge financial support from the Irish Research Council (Project No: RS/2012/152) and Maynooth University John and Pat Hume Scholarships. We thank Caroline H. Reid (Maynooth University) for helpful discussions and Dr. Gama T. Gnahore (Maynooth University) for help in generating the biosensor schematics.

Conflict of Interest

The authors declare no conflict of interest.

Keywords: Amperometry · biosensor · superoxide · real-time

[1] Y. Tian, L. Mao, T. Ohsaka, *Current Analytical Chemistry* **2006**, *2*, 51–58.
[2] K. Krumova, G. Cosa, in Singlet Oxygen: Applications in Biosciences and Nanosciences, Volume 1, Vol. 1, The Royal Society of Chemistry, **2016**, pp. 1–21.
[3] C. M. Maier, P. H. Chan, *The Neuroscientist* **2002**, *8*, 323–334.
[4] Z. Wang, D. Liu, H. Gu, A. Zhu, Y. Tian, G. Shi, *Biosensors and Bioelectronics* **2013**, *43*, 101–107.
[5] Z. Deng, Q. Rui, X. Yin, H. Liu, Y. Tian, *Analytical Chemistry* **2008**, *80*, 5839–5846.
[6] C. J. McNeil, P. Manning, *Reviews in Molecular Biotechnology* **2002**, *82*, 443–455.
[7] Y. Zhou, J. Ding, T. Liang, E. S. Abdel-Halim, L. Jiang, J.-J. Zhu, *ACS applied materials & interfaces* **2016**, *8*, 6423–6430.
[8] Y. Liu, X. Liu, Y. Liu, G. Liu, L. Ding, X. Lu, *Biosensors and Bioelectronics* **2017**, *90*, 39–45.
[9] Z. Wang, L.M. Zhang, Y. Tian, *Chinese Journal of Analytical Chemistry* **2014**, *42*, 1–9.
[10] M. Ganesana, J. S. Erlichman, S. Andreescu, *Free Radical Biology and Medicine* **2012**, *53*, 2240–2249.
[11] J. R. Harbour, M. L. Hair, *The Journal of Physical Chemistry* **1978**, *82*, 1397–1399.
[12] N. Warwar, A. Mor, R. Fluhr, R. P. Pandian, P. Kuppusamy, A. Blank, *Biophysical Journal* **2011**, *101*, 1529–1538.
[13] K. Abbas, M. Hardy, F. Poulhès, H. Karoui, P. Tordo, O. Ouari, F. Peyrot, *Free Radical Biology and Medicine* **2014**, *71*, 281–290.
[14] Y. Ohara, T. E. Peterson, D. G. Harrison, *Journal of Clinical Investigation* **1993**, *91*, 2546–2551.
[15] K. Prasad, J. Kalra, B. Bharadwaj, *British Journal of Experimental Pathology* **1989**, *70*, 463–468.
[16] S. Yamaguchi, N. Kishikawa, K. Ohyama, Y. Ohba, M. Kohno, T. Masuda, A. Takadate, K. Nakashima, N. Kuroda, *Analytica Chimica Acta* **2010**, *665*, 74–78.

[17] D. Wang, L. Zhao, L.H. Guo, H. Zhang, *Analytical Chemistry* **2014**, *86*, 10535–10539.
[18] Š. Mesároš, Ž. Vaňková, S. Grunfeld, A. Mesárošová, T. Malinski, *Analytica Chimica Acta* **1998**, *358*, 27–33.
[19] L. Campanella, G. Favero, L. Persi, M. Tomassetti, *Journal of Pharmaceutical and Biomedical Analysis* **2000**, *23*, 69–76.
[20] S. Kintzios, I. Marinopoulou, G. Moschopoulou, O. Mangana, K. Nomikou, K. Endo, I. Papanastasiou, A. Simonian, *Biosensors and Bioelectronics* **2006**, *21*, 1365–1373.
[21] K. Endo, T. Miyasaka, S. Mochizuki, S. Aoyagi, N. Himi, H. Asahara, K. Tsujioka, K. Sakai, *Sensors and Actuators B: Chemical* **2002**, *83*, 30–34.
[22] Y. Tian, L. Mao, T. Okajima, T. Ohsaka, *Biosensors and Bioelectronics* **2005**, *21*, 557–564.
[23] L. Wu, X. Zhang, J. Chen, *Journal of Electroanalytical Chemistry* **2014**, *726*, 112–118.
[24] X. Wang, M. Han, J. Bao, W. Tu, Z. Dai, *Analytica Chimica Acta* **2012**, *717*, 61–66.
[25] M. Braik, M. M. Barsan, C. Dridi, M. Ben Ali, C. M. A. Brett, *Sensors and Actuators B: Chemical* **2016**, *236*, 574–582.
[26] X. Zhu, X. Niu, H. Zhao, J. Tang, M. Lan, *Biosensors and Bioelectronics* **2015**, *67*, 79–85.
[27] C. Mateo, J. M. Palomo, G. Fernandez-Lorente, J. M. Guisan, R. Fernandez-Lafuente, *Enzyme and Microbial Technology* **2007**, *40*, 1451–1463.
[28] A. Sassolas, L. J. Blum, B. D. Leca-Bouvier, *Biotechnology Advances* **2012**, *30*, 489–511.
[29] D. R. Thévenot, K. Toth, R. A. Durst, G. S. Wilson, *Biosensors and Bioelectronics* **2001**, *16*, 121–131.
[30] R. D. O'Neill, J. P. Lowry, M. Mas, *Critical Reviews in Neurobiology* **1998**, *12*, 69–128.
[31] J. Lowry, R. O'Neill, *Encyclopedia of Sensors* **2005**, 501–524.
[32] P. Kuppusamy, J. L. Zweier, *Journal of Biological Chemistry* **1989**, *264*, 9880–9884.
[33] R. Aitken, D. Buckingham, D. Harkiss, *Journal of Reproduction and Fertility* **1993**, *97*, 441–450.
[34] N. Hamdi, J. Wang, H. G. Monbouquette, *Journal of Electroanalytical Chemistry* **2005**, *581*, 258–264.
[35] J. P. Lowry, R. D. O'Neill, *Electroanalysis* **1994**, *6*, 369–379.
[36] J. D. Craig, R. D. O'Neill, *Analyst* **2003**, *128*, 905–911.
[37] R. D. O'Neill, G. Rocchitta, C. P. McMahon, P. A. Serra, J. P. Lowry, *TrAC Trends in Analytical Chemistry* **2008**, *27*, 78–88.
[38] S. Miwa, F. L. Muller, K. B. Beckman, in *Oxidative Stress in Aging: From Model Systems to Human Diseases* (Eds.: S. Miwa, K. B. Beckman, F. L. Muller), Humana Press, Totowa, NJ, **2008**, pp. 11–35.
[39] R. Rakhit, A. Chakrabartty, Biochimica et Biophysica Acta (BBA) - Molecular Basis of Disease **2006**, 1762, 1025–1037.
[40] M. Pontie, F. Bedioui, *Analusis* **1999**, *27*, 564–569.
[41] K. L. Baker, F. B. Bolger, J. P. Lowry, *Analyst* **2015**, *140*, 3738–3745.
[42] K. L. Baker, F. B. Bolger, J. P. Lowry, *Sensors and Actuators B: Chemical* **2017**, *243*, 412–420.
[43] K. O'Brien, S. Killoran, R. O'Neill, J. Lowry, *Biosensors and Bioelectronics* **2007**, *22*, 2994–3000.
[44] E. Emregül, Analytical and Bioanalytical Chemistry **2005**, 383, 947–954.
[45] M. R. Ryan, J. P. Lowry, R. D. O'Neill, *Analyst* **1997**, *122*, 1419–1424.
[46] C. P. McMahon, G. Rocchitta, P. A. Serra, S. M. Kirwan, J. P. Lowry, R. D. O'Neill, *Analyst* **2006**, *131*, 68–72.
[47] K. Reybier, S. Zairi, N. Jaffrezic-Renault, B. Fahys, *Talanta* **2002**, *56*, 1015–1020.
[48] M. M. Andersson, R. Hatti-Kaul, *Journal of Biotechnology* **1999**, *72*, 21–31.
[49] L. Mazzaferro, J. D. Breccia, M. M. Andersson, B. Hitzmann, R. Hatti-Kaul, *International Journal of Biological Macromolecules* **2010**, *47*, 15–20.
[50] C. P. McMahon, G. Rocchitta, S. M. Kirwan, S. J. Killoran, P. A. Serra, J. P. Lowry, R. D. O'Neill, *Biosensors and Bioelectronics* **2007**, *22*, 1466–1473.
[51] J. Jezkova, E. I. Iwuoha, M. R. Smyth, K. Vytras, *Electroanalysis* **1997**, *9*, 978–984.
[52] G. B. Broun, in *Methods in Enzymology, Vol. Volume 44*, Academic Press, **1976**, pp. 263–280.
[53] P. E. M. Phillips, R. M. Wightman, *TrAC Trends in Analytical Chemistry* **2003**, *22*, 509–514.
[54] T. T. Nguyen-Boisse, J. Saulnier, N. Jaffrezic-Renault, F. Lagarde, *Sensors and Actuators B: Chemical* **2013**, *179*, 232–239.
[55] N. V. Kulagina, L. Shankar, A. C. Michael, *Analytical Chemistry* **1999**, *71*, 5093–5100.
[56] Y. Hu, G. S. Wilson, *Journal of Neurochemistry* **1997**, *68*, 1745–1752.
[57] F. Tian, A. V. Gourine, R. T. R. Huckstepp, N. Dale, *Analytica Chimica Acta* **2009**, *645*, 86–91.
[58] J. P. Lowry, M. Miele, R. D. O'Neill, M. G. Boutelle, M. Fillenz, *Journal of Neuroscience Methods* **1998**, *79*, 65–74.
[59] J. P. Lowry, K. McAteer, S. S. El Atrash, A. Duff, R. D. O'Neill, *Analytical Chemistry* **1994**, *66*, 1754–1761.
[60] F. B. Bolger, S. B. McHugh, R. Bennett, J. Li, K. Ishiwari, J. Francois, M. W. Conway, G. Gilmour, D. M. Bannerman, M. Fillenz, M. Tricklebank, J. P. Lowry, *Journal of Neuroscience Methods* **2011**, *195*, 135–142.
[61] Z. M. Zain, R. D. O'Neill, J. P. Lowry, K. W. Pierce, M. Tricklebank, A. Dewa, S. A. Ghani, *Biosensors and Bioelectronics* **2010**, *25*, 1454–1459.
[62] F. O. Brown, J. P. Lowry, *Analyst* **2003**, *128*, 700–705.
[63] M. Miele, M. Fillenz, *Journal of Neuroscience Methods* **1996**, *70*, 15–19.

Submitted: April 14, 2017
Revised: May 4, 2017
Accepted: May 8, 2017